Free Radical Biology & Medicine 51 (2011) 733–743

Contents lists available at ScienceDirect

Free Radical Biology & Medicine

journal homepage: www.elsevier.com/locate/freeradbiomed

Original Contribution

Myoglobin-H_2O_2 catalyzes the oxidation of β-ketoacids to α-dicarbonyls: Mechanism and implications in ketosis

Douglas Ganini [a], Marcelo Christoff [a], Marilyn Ehrenshaft [b], Maria B. Kadiiska [b], Ronald P. Mason [b], Etelvino J.H. Bechara [a,c,*]

[a] Departamento de Bioquímica, Instituto de Química, Universidade de São Paulo, São Paulo, SP, Brazil
[b] Free Radical Metabolism Group, Laboratory of Toxicology and Pharmacology, National Institute of Environmental Health Sciences, NIH, Research Triangle Park, NC 27709, USA
[c] Departamento de Ciências Exatas e da Terra, Instituto de Ciências Ambientais, Químicas e Farmacêuticas, Universidade Federal de São Paulo, Diadema, SP, Brazil

ARTICLE INFO

Article history:
Received 1 March 2011
Revised 14 April 2011
Accepted 2 May 2011
Available online 8 May 2011

Keywords:
Myoglobin
Acetoacetate
2-Methylacetoacetate
Free radicals
Triplet carbonyls
Methylglyoxal
Diacetyl
Ketosis

ABSTRACT

Acetoacetate (AA) and 2-methylacetoacetate (MAA) are accumulated in metabolic disorders such as diabetes and isoleucinemia. Here we examine the mechanism of AA and MAA aerobic oxidation initiated by myoglobin (Mb)/H_2O_2. We propose a chemiluminescent route involving a dioxetanone intermediate whose thermolysis yields triplet α-dicarbonyl species (methylglyoxal and diacetyl). The observed ultraweak chemiluminescence increased linearly on raising the concentration of either Mb (10–500 μM) or AA (10–100 mM). Oxygen uptake studies revealed that MAA is almost a 100-fold more reactive than AA. EPR spin-trapping studies with MNP/MAA revealed the intermediacy of an α-carbon-centered radical and acetyl radical. The latter radical, probably derived from triplet diacetyl, is totally suppressed by sorbate, a well-known quencher of triplet carbonyls. Furthermore, an EPR signal assignable to MNP-AA$^{\bullet}$ adduct was observed and confirmed by isotope effects. Oxygen consumption and α-dicarbonyl yield were shown to be dependent on AA or MAA concentrations (1–50 mM) and on H_2O_2 or *tert*-butOOH added to the Mb-containing reaction mixtures. That ferrylMb is involved in a peroxidase cycle acting on the substrates is suggested by the reaction pH profiles and immunospin-trapping experiments. The generation of radicals and triplet dicarbonyl products by Mb/H_2O_2/β-ketoacids may contribute to the adverse health effects of ketogenic unbalance.

Introduction

Acetoacetate (AA) is a carbohydrate, protein, and lipid catabolite that is normally found in human plasma at concentrations below 0.5 mM, but can reach 6–10 mM during ketosis, a characteristic of diabetes *mellitus* types 1 and 2 [1], strenuous physical exercise [2], and the Atkins diet [3]. Another β-ketoacid, 2-methylacetoacetate (MAA) accumulates in isoleucinemic patients, whose 2-methylacetoacetyl-CoA thiolase is defective [4], leading to massive urinary excretion of MAA, triglylglycine, and 2-methyl-3-hydroxybutyrate [5]. Isoleucinemic patients are characterized by recurrent ketoacidosis, lethargy, vomiting, and usually manifest mental retardation, convulsions, and coma [6].

AA is reportedly toxic to cells in culture due to generation of free radicals and activation of pro-oxidant signaling pathways. For example, exposure of monocyte cultures to AA (2–3 mM) results in higher secretion of tumor necrosis factor-α (TNF-α) and depletion of reduced glutathione (GSH) [7,8], and in higher interleukin-6 secretion when in the presence of phorbol 12-myristate 13-acetate [9]. Mitogen-activated protein kinase (MAPK) increases in AA (0.5–20 mM)-treated primary rat hepatocyte cultures [10], and endothelial cells exposed to AA (5–20 mM) display higher levels of malondialdehyde and undergo growth inhibition [11]. Paradoxically, AA was also shown to exhibit antioxidant properties, for example, in neurons stressed by glutamate or hypoxia [12]. In addition, AA increases the contractile performance of stunned myocardium by acting as a β-adrenergic inotropic substance due to its utilization as carbon fuel [13] and NAD(P)$^+$-linked substrate [14].

Abbreviations: AA, acetoacetate; AGEs, advanced glycated end products; CAT, catalase; DMPO, 5,5′-dimethyl-1-pyrroline *N*-oxide; ELISA, enzyme-linked immunosorbent assay; EPR, electron paramagnetic resonance; FOX1, ferrous oxidation of xylenol orange; GSH, reduced glutathione; HPLC, high performance liquid chromatography; HRP, horseradish peroxidase; MAA, 2-methylacetoacetate; Mb, myoglobin; MNP, methylnitrosopropane; NKκβ, nuclear factor κβ; OPD, *o*-phenylenediamine; RAGE, AGE receptor; SOD, superoxide dismutase; *tert*-ButOOH, *tert*-butyl hydroperoxide; TNF-α, tumor necrosis factor α.

* Corresponding author at: Departamento de Ciências Exatas e da Terra, Instituto de Ciências Ambientais, Químicas e Farmacêuticas, Universidade Federal de São Paulo, Rua Prof. Artur Riedel, 275, 09972–270 Diadema, SP, Brazil. Fax: +55 11 4043 6428.
E-mail address: ejhbechara@gmail.com (E.J.H. Bechara).

0891-5849 © 2011 Elsevier Inc. Open access under the Elsevier OA license.
doi:10.1016/j.freeradbiomed.2011.05.002

It has long been known that myoglobin catalyzes the chemiluminescent oxidation of AA to formate and triplet methylglyoxal, probably via a dioxetane intermediate [15]. Myeloperoxidase [16] and, more recently, peroxynitrite [17] were also shown to trigger the oxidation of β-ketoacids, in the latter case demonstrated to yield methylglyoxal and diacetyl from AA and MAA as substrates, respectively (Scheme 1). Noteworthy in this regard is that clinical studies with diabetic patients show a high correlation between plasma levels of AA and methylglyoxal, but not glucose [18].

Reactive carbonyl species such as methylglyoxal, an α-oxoaldehyde, can aggregate proteins and generate protein and DNA adducts [19], reportedly leading to activation of pro-oxidant signaling cascades [20], cellular malfunction, and aging [21,22]. Various pathological states, such as diabetes type I and II, cardiovascular diseases, inflammation, and chronic renal failure are shown to be related to accumulation of methylglyoxal and carbonyl protein adducts, collectively named "advanced glycated end products" (AGEs) [23]. The progression of diabetic micro- and macrovascular manifestations such as retinopathy and chronic kidney failure is shown in different animal models and humans to be correlated to indexes of AGEs such as carboxyethyl-ε-amine-lysine (CML), pentosidine, glyoxal-derived lysine dimer, and methylglyoxal-derived lysine dimer [24–27]. Recently, a receptor for AGEs, RAGE, was characterized and described to be directly associated with the initiation of microvascular diseases [28]. Soluble AGEs, such as the well-characterized CML, induce receptor expression and lead to the activation of signaling cascades through MAPK and NFκβ [29].

Here, we aim to clarify the mechanism of the Mb/peroxide-catalyzed oxidation of AA and MAA through free radicals to methylglyoxal and diacetyl, respectively, in normally aerated buffer (Scheme 2). This may shed light on the molecular bases of the clinical complications of ketoacidosis and rhabdomyolysis. Acting as a peroxidase in the presence of H_2O_2, the very unstable Compound I form of Mb is stabilized by electron transfer from the heme moiety to the Tyr103 residue, giving rise to Mb Compound II [30–32]. One or more of these species is expected to oxidize AA or MAA yielding a resonance-stabilized enoyl radical ($AA^{\bullet}$ or $MAA^{\bullet}$) (Scheme 2). Reaction of these radicals with dioxygen would form the corresponding alkylperoxyl radicals that can propagate the chain reaction to the α-hydroperoxides AAOOH or MAAOOH. The hydroperoxides might then undergo cyclization to dioxetane intermediates followed by their thermolysis to methylglyoxal or diacetyl products in the triplet state. Both ground state [19,20] and excited state [33] α-dicarbonyl products are very reactive toward proteins, DNA, and a wide spectrum of biomolecules. Myoglobin is therefore expected to be damaged by the AA and MAA radical intermediates and dicarbonyl products. In this regard, we emphasize here that the reaction of Mb with lipid peroxides in kidneys of rats intramuscularly injected with glycerol seems to contribute to the acute kidney failure caused by rhabdomyolysis [34].

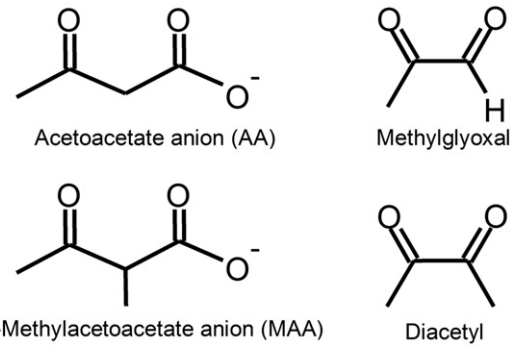

Scheme 1. Chemical structures of acetoacetate (AA) and 2-methylacetoacetate (MAA) anions and of their oxidation products: methylglyoxal and diacetyl, respectively.

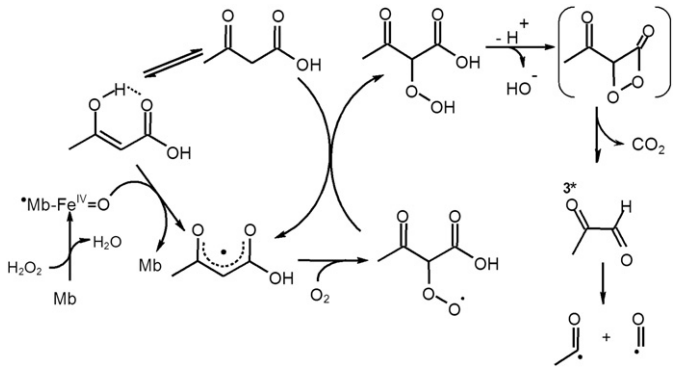

Scheme 2. Proposed reaction mechanism for the chemiluminescent oxidation of AA by Mb/H_2O_2.

Materials and methods

Reagents

Ethyl acetoacetate and ethyl 3-methylacetoacetate were from Aldrich Co. (Saint Louis, MO, USA). Glyoxal (40%), methylglyoxal, diacetyl, quinoxalinol, 2-methylquinoxaline, 2,3-dimethyquinoxaline, xylenol orange, horse myoglobin (Mb), sorbic acid, sodium pyruvate, glucose oxidase (from *Aspergillus niger*), *o*-phenylenediamine (OPD), butanone, methylnitrosopropane (MNP), catalase (CAT), Cu,Zn-superoxide dismutase (SOD) (from bovine erythrocytes), and 70% *tert*-butyl hydroperoxide were from Sigma Co. (St. Louis, MO, USA). Hydrogen peroxide (30%), methanol, acetonitrile, phosphoric acid (85%), acetic acid, HPLC grade solvents, and salts used for buffer preparation of the highest purity available were from Merck Co. (Darmstadt, Germany). DMPO was from Dojindo Co. (Kumamoto, Japan). All solutions were prepared with water from MilliQ or PicoPure systems. Phosphate buffers were treated with Chelex before use. Ethyl acetoacetate and ethyl 3-methylacetoacetate were distilled, aliquoted, and kept at −20 °C until use. H_2O_2 solutions ($\varepsilon_{240nm} = 0.0436\ mM^{-1}\ cm^{-1}$ [35]) were prepared in water.

Sodium AA and sodium MAA were prepared daily by saponification of ethyl acetoacetate or ethyl 3-methylacetoacetate 1.0 mol L^{-1} in water with 20% excess of NaOH for 1 h at 25 °C [36]. The solutions were neutralized with HCl 2.0 mol L^{-1} and diluted to 0.25 mol L^{-1} before use.

Myoglobin preparation

Ferri- and ferromyoglobin were prepared by the addition of potassium ferricyanide or sodium dithionite 10% (w/w), respectively, to the protein solution (50 mg mL^{-1}) in phosphate buffer 20 mM, pH 7.0 equilibrated with N_2 [37]. After 10 min the protein was desalted in a diethylammonium ethyl-cellulose column equilibrated with phosphate buffer 20 mM, pH 7.0. The pooled protein fraction was chromatographed in a Sephadex G25 column, eluted with phosphate buffer 20 mM, pH 7.4. The ferri- and ferromyoglobin concentrations were determined ($\epsilon_{630} = 2.1\ mM^{-1}\ cm^{-1}$ and $\epsilon_{580} = 14.4\ mM^{-1}\ cm^{-1}$, respectively [30]), and aliquots were stored at −20 °C until use. Ferrylmyoglobin was determined in reaction mixtures as described by Giulivi and Cadenas [30] using a Varian, 50 BIO UV-VIS spectrophotometer. Unless otherwise stated, all experiments were performed with ferrimyoglobin, abbreviated here as Mb. The reactions were carried on under constant stirring in closed vials.

Light emission measurements

Ultraweak chemiluminescence was detected in a Hamamatsu, Model TVC 767, photocounter coupled to a Thorn EMI, Model 9658 AM, photomultiplier kept at −8 °C by an EMI, Model FACT50, thermoelectric refrigerator.

Myoglobin immunospin-trapping experiments

Samples were prepared in 100 mM phosphate buffer, pH 7.4, containing 10 μM Mb, 50 mM DMPO, with (i) 1.0–50 mM AA or MAA and 100 μM H_2O_2, or (ii) 10 mM AA or MAA and 1.0 μM–1.0 mM H_2O_2. The reaction was stopped after 2 h by the addition of 250 U mL^{-1} CAT. After 5 min at 25 °C, the samples were diluted to (i) ice-cold buffer for denaturating gel electrophoresis (1.25 μg of protein per lane) or (ii) binding buffer for ELISA (2.25 μg of protein per well in 200 mM carbonate buffer, pH 9.4).

Denaturing gel eletrophoresis was run with supplies from a NuPAGE system (Invitrogen Co., USA) according to the manufacturer's instructions.

Western blotting and ELISA were conducted using standard procedures. Rabbit primary antibody anti-DMPO nitrone adduct, polyclonal, was used at 1:5000 for Western blot (2 h at 25 °C) and ELISA (1 h at 37 °C). Anti-rabbit secondary antibody, alkaline phosphatase conjugated (Santa Cruz), was used at 1:500 for ELISA (1 h at 37 °C), and anti-rabbit, IRDye 800CW conjugated (Li-Cor), was used at 1:10,000 for Western blot (1 h at 25 °C).

CDP-Star (Tropix) was used as an alkaline phosphatase chemiluminescent substrate for the ELISA development, and the membranes were scanned using the 800 nm laser of a Li-Cor infrared scanner Odyssey for the Western blot detection.

Oxygen consumption

Oxygen uptake was monitored using a Clark-type electrode system from Hansatech (Oxygraph system). The O_2 concentrations were assumed to be 240 and 210 μM under normal atmosphere pressure at 25 and 37 °C, respectively [38].

EPR spin-trapping studies

EPR spectra were obtained in a Bruker EMX spectrometer with a High Q cavity at 25 °C. Spectra were recorded 3 min after the addition of H_2O_2. Spectra were acquired using the software WinEPR. Instrumental conditions were as follows: microwave power 20 mW, time constant 83 ms, sweep time 1 G s^{-1}, modulation of amplitude 0.5 G and gain 2.0×10^4. The spin-trapping agent MNP was prepared in an amber vial using acetonitrile as solvent [39]. The solution was prepared 3 h before use. Samples deprived of β-ketoacids did not display any MNP adduct signal, possibly originated by oxidation of the solvent by Mb and H_2O_2. The experimental hyperfine splitting constants are reproducible within 5% error. Spectral simulations were made using the free software WinSim, version 0.96.

Determination of α-dicarbonyls

α-Dicarbonyl products from AA or MAA/Mb/H_2O_2 were derivatized with *o*-phenylenediamine and the resulting quinoxalines analyzed by HPLC as follows [40,41]. Before addition of OPD (0.038%, w/v, prepared in water), the pH of samples obtained from the reaction mixture in phosphate buffer 0.10 M, pH 7.4 was adjusted with acetic acid (62 mM) to about 5.0. The samples were incubated with OPD for 1 h under continuous agitation at 60 °C, and filtered through 0.45-μm PVDF-syringe filters (Millipore) to be injected into the HPLC. Twenty microliters of OPD-treated solutions was injected into a Model 515 Waters apparatus equipped with two pumps, an automatic injector (Model 717 Plus) and a photodiode array detector (Model 996), with a C18 precolumn (0.5 cm × 4.6 mm) and column (25 cm × 4.6 mm), particle size of 50 μm (Supelco).

Isocratic separation was employed using as a mobile phase 20 mM acetate buffer, pH 4.2, added to acetonitrile 6:4 (V/V). Better resolution was achieved in the gradient mode using 30 to 90% methanol in 20 mM acetate buffer, pH 4.2, over 30 min, followed by the initial conditions for 5 min.

Quinoxaline HPLC peaks were characterized by the retention times and the absorption spectra of quinoxalines reported elsewhere [42]. Peaks were quantified using a standard curve (R^2>0.995) obtained with samples prepared of 5.0 μM–5 mM methylglyoxal or diacetyl treated with OPD by the same procedure used for the reaction mixtures. Chromatograms extracted from the data acquired by the photodiode array detector at 314 nm were used for peak integration and quantification.

Acetoacetate determination

Acetoacetate was determined according to Walker [43], modified as follows. The diazonium salt of *p*-nitroaniline (0.04%, w/v) in 70 mM acetate buffer, pH 5.5, reacts with AA yielding an orange adduct that was measured at 450 nm for 5 min. The curved slope was used to calculate the concentration of AA in the reaction sample. The high assay sensitivity allowed calculating AA consumption as the

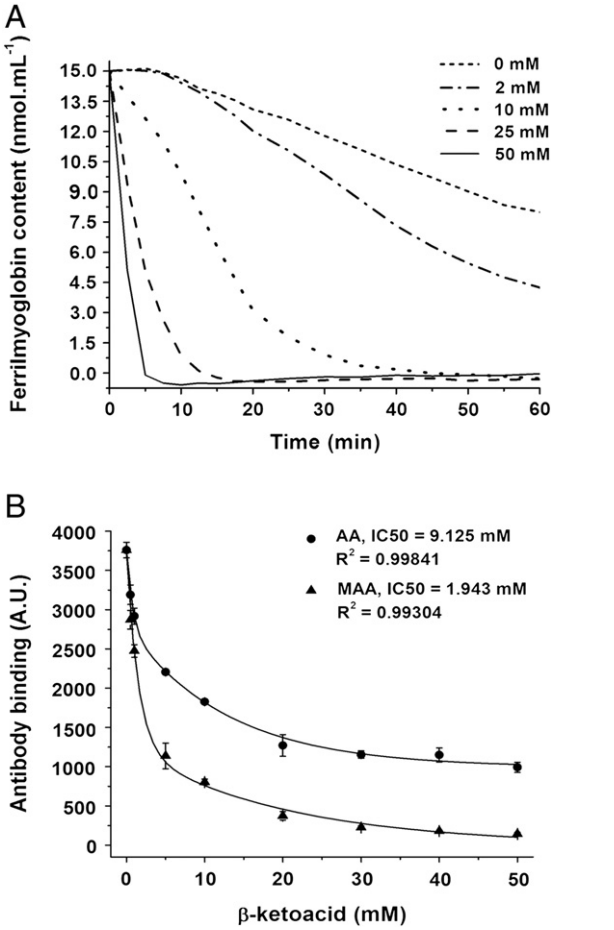

Fig. 1. Peroxidase activity of myoglobin/H_2O_2 on AA and MAA substrates in normally aerated 100 mM phosphate buffer, pH 7.4. (A) Ferrylmyoglobin (15 μM) decay induced by MAA (2.0–50 mM). (B) Abatement of DMPO-Tyr103 Mb yield promoted by AA and MAA (0.50–50 mM). Ratio Mb:H_2O_2 is 1:1 in A and 1:10 in B. Experimental conditions are described under Materials and methods. Data are representative of at least 3 independent experiments.

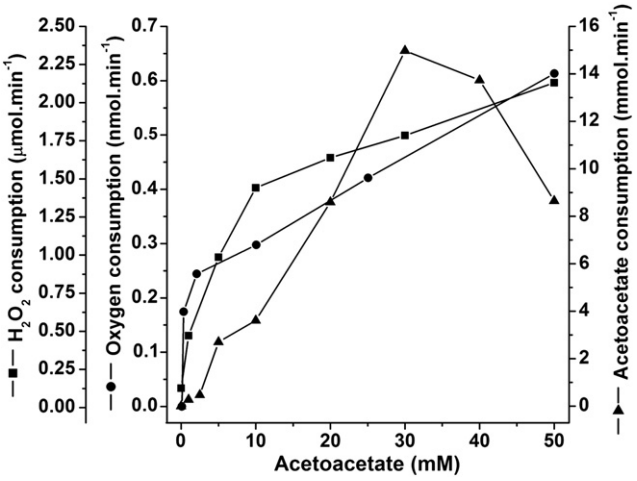

Fig. 2. Aerobic oxidation of AA catalyzed by Mb on adding H_2O_2 accompanied by O_2 (●), H_2O_2 (■), and AA (▲) consumption. Reactions were prepared in 100 mM phosphate buffer, pH 7.4. Other experimental conditions are described under Materials and methods. Data are representative of three independent experiments.

difference between AA concentration in aliquots prior to and after H_2O_2 addition to the reaction mixtures.

MAA, glyoxal, diacetyl, methylglyoxal, sodium pyruvate, and sodium oxalate (5 mM each) did not result in any absorbance increase at 450 nm.

H_2O_2 determination

Hydrogen peroxide was determined every 2 min by the ferrous oxidation of xylenol orange (FOX1) method [44]. Notably, iron ions liberated by Mb in the presence of hydroperoxides could result in overestimation of the FOX assay [45]; however, addition of CAT (10 U mL^{-1}) 5 min prior to the H_2O_2 assay completely abolishes the FOX signal.

Results

Spectrophotometric and immunospin-trapping studies

To demonstrate that MAA and AA behave as substrates for ferrylMb acting as a peroxidase, heme hyperoxidation and Tyr 103 primary protein radical formation were monitored by a spectrophotometric assay of ferrylMb and an immunospin-trapping experiment (Fig. 1). Both β-ketoacids—AA (2.0–50 mM), used in ferrylMb evaluation, and AA or MAA (0.50–50 mM), used in the immunospin-trapping experiments—were shown to be electron donors in phosphate buffer, pH 7.4, to Mb intermediates generated on addition of H_2O_2. Myoglobin and H_2O_2 were tested at ratios of 1:1 for measuring ferrylMb content and 1:10 in the immunospin-trapping experiments. The immunospin-trapping studies showed that MAA is roughly 5-fold more effective than AA in inhibiting the antibody binding, revealing a higher reactivity for MAA. This difference is predicted by the lower oxidation potential of the enol forms of α-alkylated β-diketones and β-ketoesters as compared to their dealkylated homologues [46].

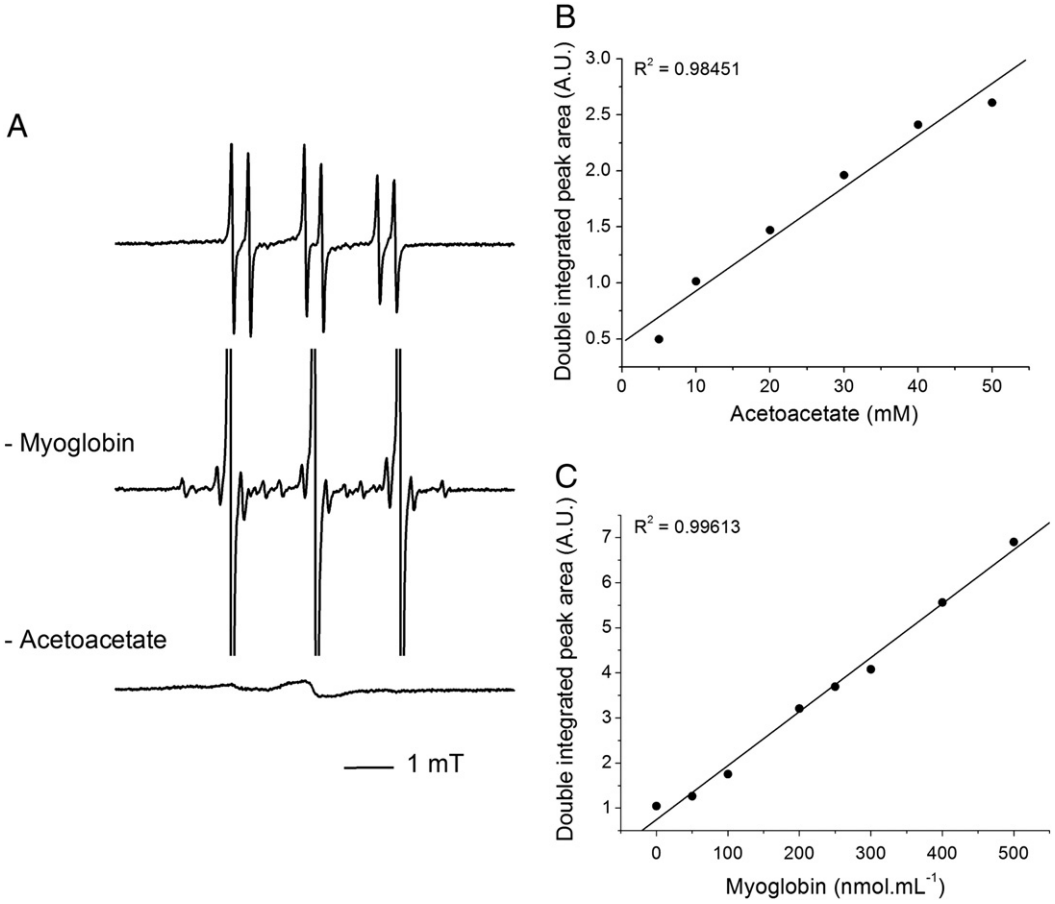

Fig. 3. EPR spin-trapping experiments with MNP, AA, and Mb in the presence of H_2O_2. The 6-line signal of the putative MNP-AA$^{\bullet}$ adduct is detected in the presence of both Mb (250 μM) and AA (50 mM), MNP 50 mM (A), and its doubly integrated area responds linearly to the reagent concentrations (B and C). Experimental conditions are described under Materials and methods.

Reaction kinetics as a function of AA concentration

Acetoacetate oxidation by Mb/H_2O_2 was accompanied by H_2O_2, O_2, and AA consumption (Fig. 2). Consumption of H_2O_2 by Mb and uptake of O_2 by AA were roughly correlated and exhibited a biphasical increase as a function of AA concentration. The exponential consumption of both O_2 and H_2O_2 occurred at low AA concentrations, but was followed by a slower near linear consumption above 10 mM.

EPR spin-trapping studies

In EPR spin trapping with MNP, the Mb/H_2O_2/AA reaction mixtures displayed a 6-line spectrum with coupling constants $a^N = 1.46$ mT and $a^H_\beta = 0.33$ mT assignable to an MNP-secondary carbon-centered radical adduct (Fig. 3A). The doubly integrated area of the signal increased on raising the concentration of both Mb (50–500 μM) and AA (5–50 mM) (Figs. 3B and C). The hyperfine coupling constants in the EPR spectral simulation of this MNP-radical adduct are similar to those found by Mottley and Robinson [47] for the acetylacetone oxidation by HRP/H_2O_2 ($a^N = 1.46$ mT and $a^H_\beta = 0.34$ mT) ascribed to -$^{\bullet}$CH-, vicinal to the two carbonyl electron-withdrawing groups. Superoxide anion radical, eventually generated by electron transfer from AA enoyl radical intermediate to O_2 as suggested by Jain et al. [11], is not involved in the chain reaction, as indicated by the absence of an SOD (4000 U mL^{-1}) effect (data not shown). Indeed, considerable evidence reveals that monoenoyl radicals like AA$^{\bullet}$ tend to insert molecular oxygen to form an alkylperoxyl radical intermediate (AAOO$^{\bullet}$) and ultimately a dioxetane by cyclization, whereas dienoyl radicals and semiquinones are prone to electron transfer to O_2 yielding $O_2^{\bullet-}$ radical and an α-dicarbonyl product or a quinone, respectively [48].

Using ^{13}C-enriched AA, along with spectral simulations, it was possible to unequivocally identify the 6-line MNP adduct signal as derived from the AA radical centered on C2 (Fig. 4).

When MAA was investigated as the substrate for the Mb/H_2O_2 system, two triplet MNP radical adducts were detected by EPR. The signal with $a^N = 0.83$ mT can be ascribed to the MNP adduct with

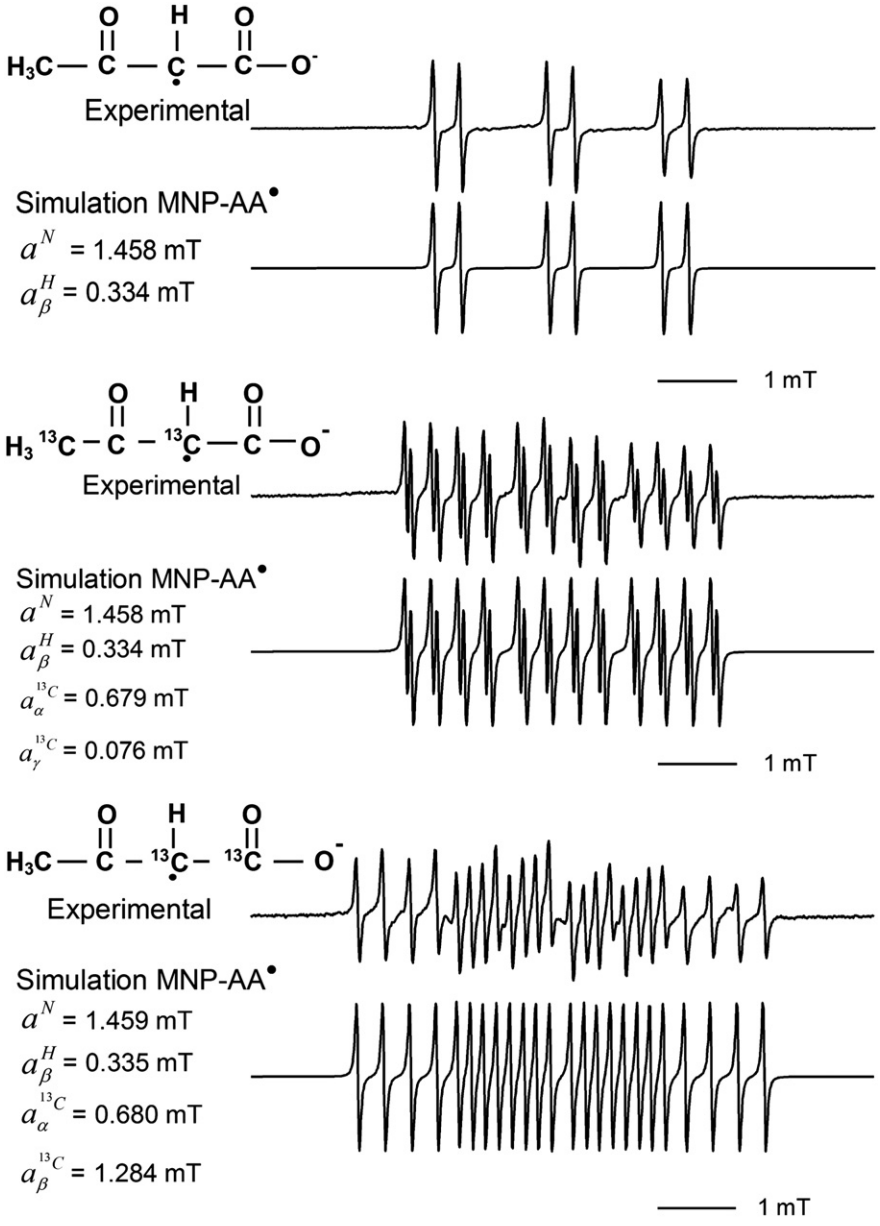

Fig. 4. EPR spectra of MNP-AA$^{\bullet}$ radical adduct assigned to the AA secondary carbon-centered radical. Reaction mixture: 100 mM MNP, and 50 mM ^{13}C-enriched AA, 500 μM Mb and 5 mM H_2O_2 in aerated 100 mM phosphate buffer, pH 7.4, at 25 °C. Other experimental conditions were as shown under Materials and methods.

acetyl radical, and the other ($a^N = 1.54$ mT) to one derived from a tertiary carbon-centered radical (Fig. 5). With regard to the detection of an acetyl radical MNP adduct in the reaction mixture, it is worth noting similar previous work carried out with 3-methylacetoacetone/HRP [46] and ethyl 2-methylacetoacetate/peroxynitrite [17]. Therein, the intermediacy of a putative MNP adduct with an acetyl radical derived from α-cleavage of triplet diacetyl formed by the thermolysis of a hypothetical dioxetane intermediate was demonstrated as well.

Product analysis associated with ferrylmyoglobin intermediacy

Two experimental protocols were used to demonstrate and quantify the generation of methylglyoxal and diacetyl by AA and MAA oxidation, respectively, mediated by the peroxidase activity of Mb. First, H_2O_2 was produced continuously by glucose (5 mM)/glucose oxidase (GOX) (1–500 mU mL^{-1}) added to the buffer. Diacetyl and methylglyoxal were found in the spent reaction mixtures of MAA and AA, respectively, in a dose-dependent fashion. At lower GOX concentrations (1–10 mU mL^{-1}), the yield of α-dicarbonyl products increases linearly on raising the β-ketoacid concentration (Fig. 6). Furthermore, under identical experimental conditions, the yield of diacetyl product was about 9-fold that of methylglyoxal, thereby confirming the higher reactivity of MAA due to the electronic effect of the α-methyl substituent. Accordingly, the rate of oxygen uptake by the MAA/Mb system was about about 9 times faster than with AA when H_2O_2 generated by glucose/GOX was replaced by a bolus addition of *tert*-butOOH (not shown). Because methylglyoxal can strongly bind to proteins, its concentration in the Mb-containing reaction mixture is probably underestimated.

A second protocol for determining products consisted of the addition of H_2O_2 at various concentrations to the Mb/β-ketoacid-containing buffer (Fig. 7). Maximal amounts of the α-dicarbonyl product were found with 1:25 Mb:H_2O_2. Under these conditions, the diacetyl yield from MAA oxidation was almost 60 times higher than that of methylglyoxal obtained from AA. Interestingly, lower yields of α-dicarbonyl products were found when the highest

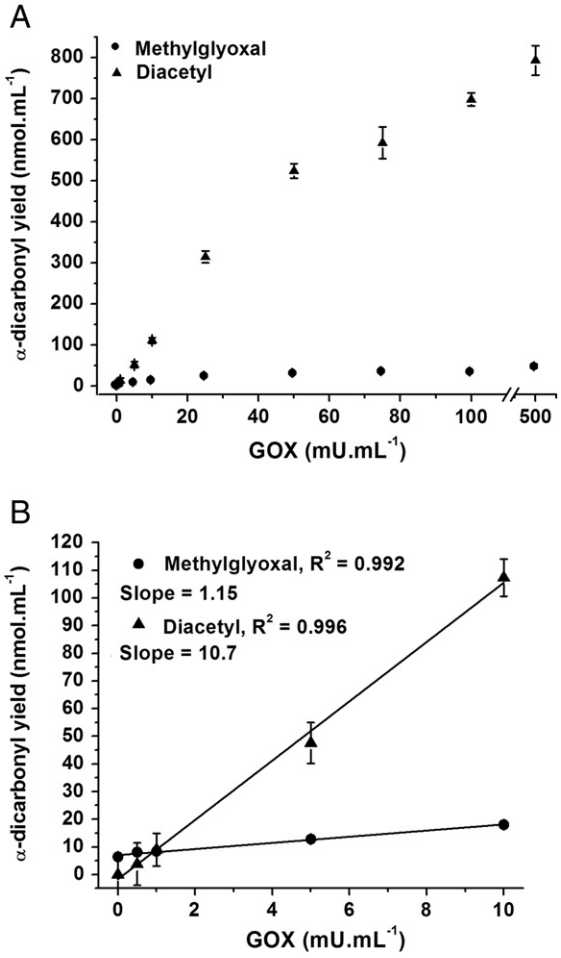

Fig. 6. Effect of H_2O_2 concentration produced by the glucose/GOX system on the yields of methylglyoxal and diacetyl produced by AA and MAA, respectively, on treatment with Mb. Reaction mixture: 5.0 mM glucose, 50 mM AA or MAA, and 50 μM Mb in aerated 100 mM phosphate buffer, pH 7.4, stirred for 2 h at 25 °C in closed vials.

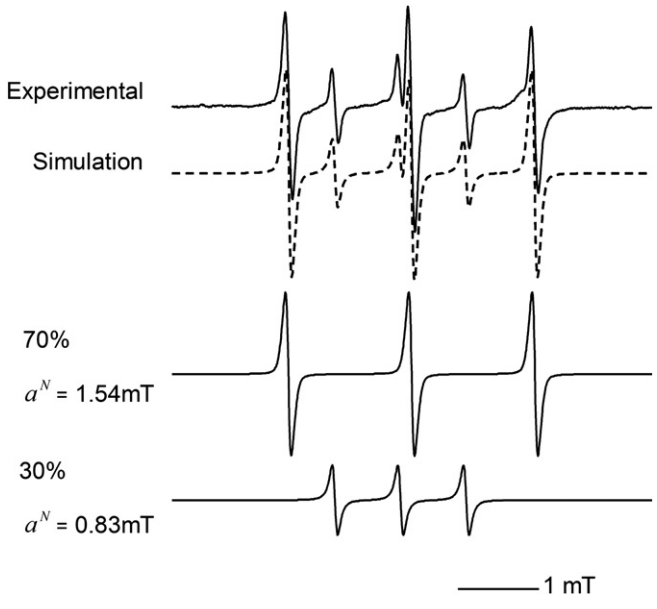

Fig. 5. EPR spin-trapping experiments using MAA as substrate for the peroxidase-acting Mb/H_2O_2 system. Experimental conditions: MNP (100 mM), MAA (50 mM), and Mb (250 μM) in the presence of H_2O_2 (1:10, 2.5 mM). Other experimental details were as shown under Materials and methods.

concentrations of H_2O_2 were used (1:50 and 1:100). In agreement, the amplitude of the MNP spin-trapping signal of AA was suppressed in a dose-dependent manner when catalase (0.16–400 U mL^{-1}) was added (data not shown). Taken together, these results indicate that the substrates undergo oxidation mediated by the redox cycling of holoMb, and not from iron or heme released by the protein.

To confirm participation of ferrylMb as the primary MAA oxidant, the pH profiles (pH 5.8 – 8.0) of oxygen consumption (Fig. 8A) and diacetyl production (Fig. 8B) were traced using MAA and Mb/H_2O_2 1:1. Ferrylmyoglobin is known to be more reactive at lower pH [34,49]. Both parameters were shown to decrease exponentially on raising the pH and to be strongly correlated. These findings support the involvement of ferrylMb in electron abstraction from MAA yielding the MAA$^{\bullet}$ radical, thereby initiating the MAAOO$^{\bullet}$-propagated oxidation of the substrate by dissolved molecular oxygen and ultimately producing diacetyl.

In order to further demonstrate a direct connection between ferrylMb and one-electron oxidation of AA and MAA, the double integrated EPR peak areas for AA$^{\bullet}$, MAA$^{\bullet}$, and acetyl adducts with MNP were studied as a function of the ratio Mb:H_2O_2 (Fig. 9). The highest radical concentrations were found for a ratio of Mb:H_2O_2 1:25. Higher peroxide concentrations led to a decrease in the signal area for the radical adducts, probably due to Mb oxidative degradation. Altogether, the areas of the radical adducts, pH profile data, and α-dicarbonyl yields are consistent with a catalytic peroxidase activity of Mb.

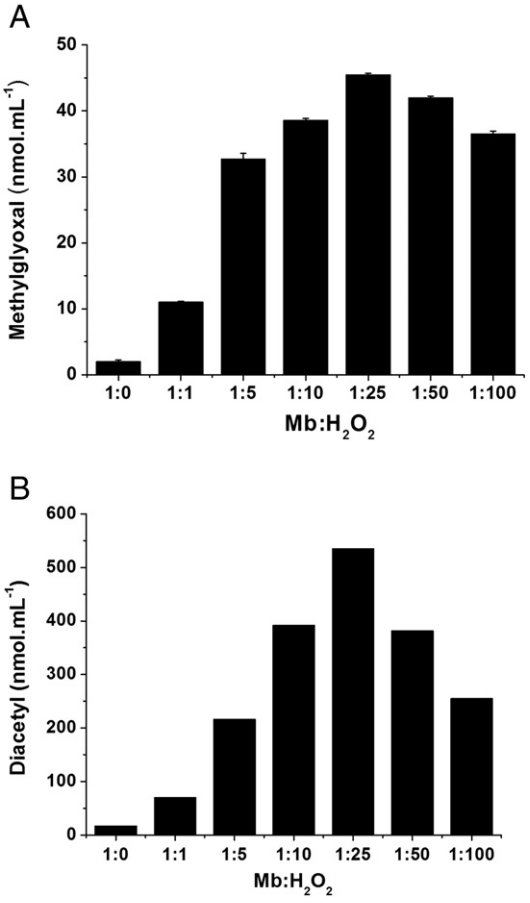

Fig. 7. Yield of methylglyoxal (A) and diacetyl (B) treated with Mb/H_2O_2. Reaction mixture: AA (A, 50 mM) and MAA (B, 50 mM) with Mb (A, 50 μM; and B, 250 μM) treated with H_2O_2 at various ratios of $Mb:H_2O_2$, in 100 mM phosphate buffer, pH 7.4, at 37 °C. Data are representative of three independent experiments.

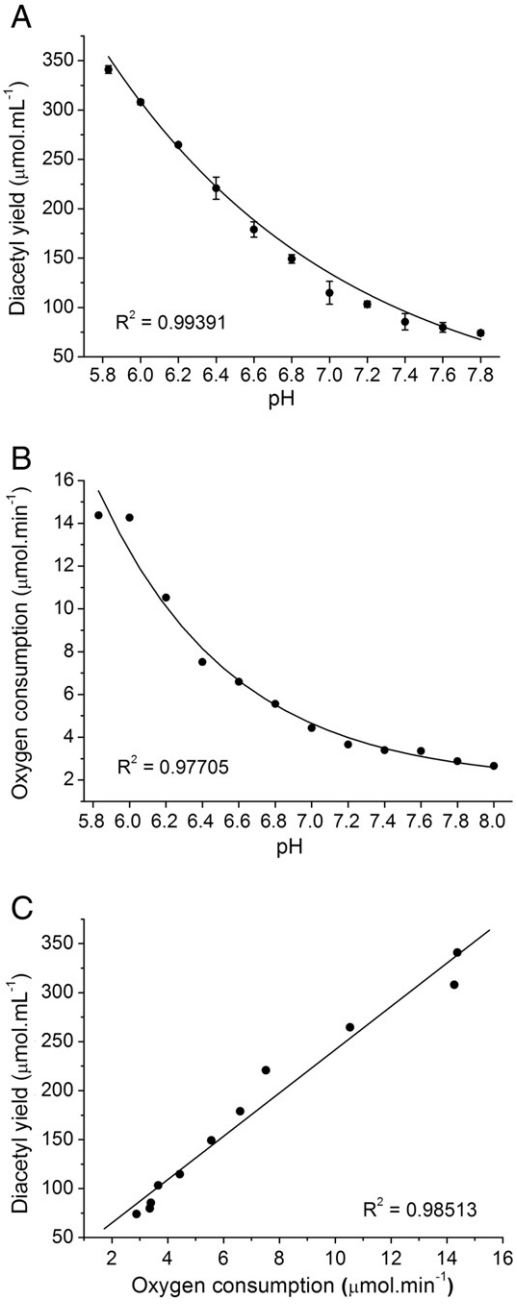

Fig. 8. pH profile of oxygen consumption and diacetyl production by MAA treated with Mb/H_2O_2. Oxygen consumption (A) and diacetyl yield (B) were determined for MAA (20 mM) treated with Mb (50 μM) in the presence of H_2O_2 (500 μM) in phosphate buffer at various pHs. Panel C depicts the correlation between the extent of oxygen uptake and diacetyl production. Other experimental conditions are described under Materials and methods.

Chemiluminescence studies

To investigate whether the oxidation of β-ketoacids indeed proceeds via a dioxetane intermediate, whose thermal cleavage yields electronically excited triplet products [33], the AA or MAA/Mb/H_2O_2-containing reaction mixtures were examined in a highly sensitive photocounter for ultraweak chemiluminescence emission (Fig. 10). Alkyl-substituted dioxetanes and dioxetanones like the hypothetical AA and MAA-derived peroxide intermediates have long been known to cleave into two carbonyl products, one of them predominantly in the triplet, phosphorescent state [33,50,51,58]. Triplet carbonyls are efficiently quenched by dissolved (triplet) molecular oxygen and thermally deactivated by solvent molecules, hence the detection of ultraweak direct chemiluminescence.

Although very weak, the intensity of light emission detected in the photocounter from the AA/Mb/H_2O_2 system was strongly correlated to the concentration of AA or Mb added in the reaction mixture (Figs. 10A–C). Because (i) methylglyoxal is the product expected from the homolysis of the hypothetical 1,2-dioxetanone derived from AA cleavage and (ii) the reaction is chemiluminescent, it is conceivable that the reaction emitter is indeed triplet methylglyoxal. If this actually happens, then triplet methylglyoxal should undergo α-cleavage (Norrish Type I reaction) yielding acetyl radical, as noted above in the EPR spin-trapping studies. Suppression of the MNP-acetyl radical adduct signal on addition of sorbate, a diffusional triplet carbonyl quencher [52], was accordingly observed when using MAA as a substrate for Mb/H_2O_2 (Fig. 10D). The EPR signal attributed to the MNP-acetyl radical adduct was affected, whereas that derived from the MAA$^{\bullet}$ intermediate was not. Furthermore, addition of sorbate did not interfere with ferrylMb generation or the ferrylMb reaction with MAA (data not shown).

Discussion

Acetoacetate and MAA are two β-ketoacid catabolites long known to be elevated at millimolar concentrations in the plasma of individuals exhibiting ketoacidoses resulting from such conditions as diabetes, fasting, and protein- and fat-rich diets. They are shown here to undergo chemiluminescent myoglobin/H_2O_2-catalyzed oxidation in normally aerated phosphate buffer, pH 7.4, yielding methylglyoxal

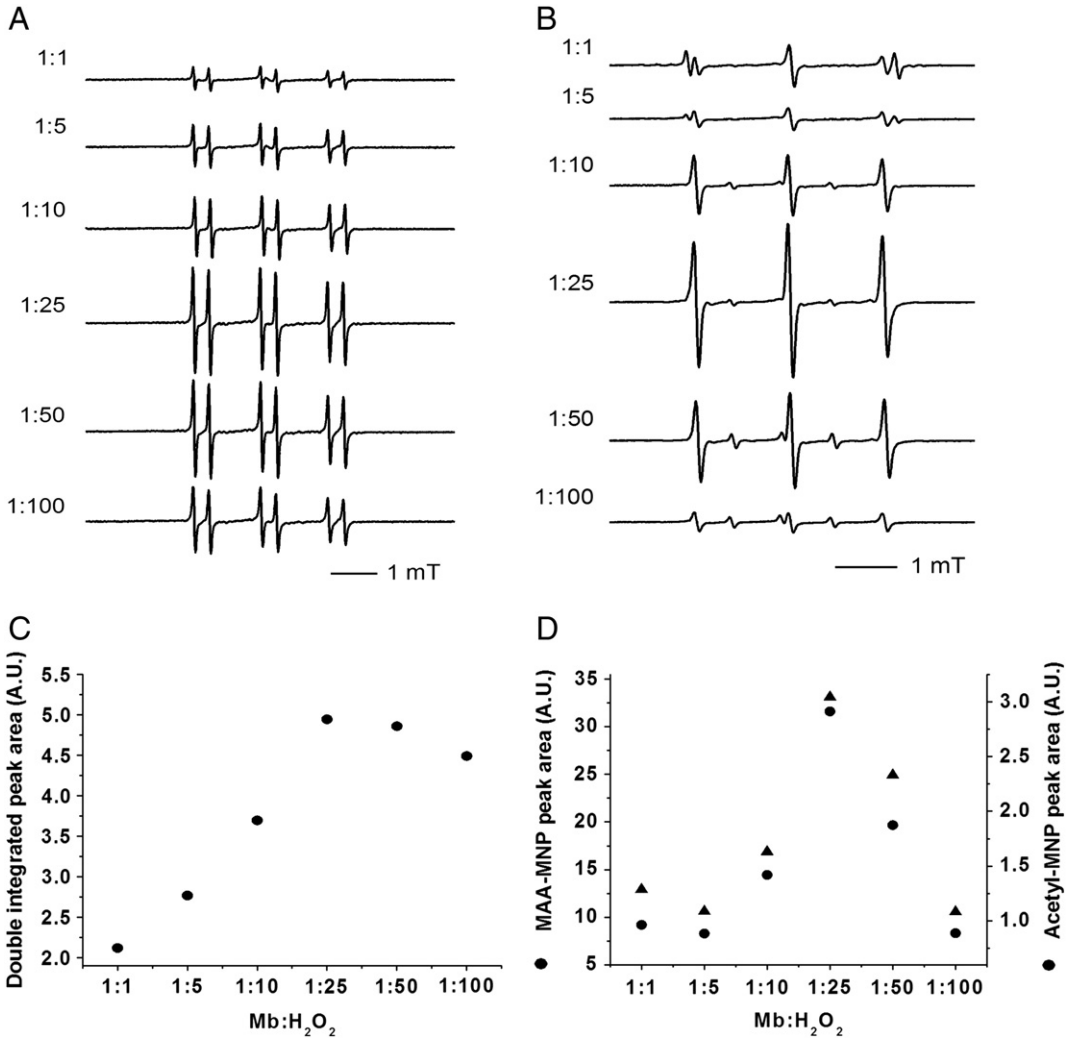

Fig. 9. EPR spin-trapping studies of the effect of the Mb:H_2O_2 concentration ratio on the oxidation of AA and MAA. Spectra were traced for reaction mixtures containing 25 mM MNP and (A) AA or (B) MAA (50 mM) treated with increasing ratios of Mb (25 μM):H_2O_2. (C and D) Dependence of the doubly integrated areas for the peaks attributed to $AA^{\bullet}$ or $MAA^{\bullet}$ (plus MNP-acetyl radical adduct in the latter case), respectively, on the Mb:H_2O_2 ratio. See Figs. 3–5 for EPR radical signal assignments.

and diacetyl, respectively, as final products. Evidence is provided here in favor of a reaction mechanism (Scheme 2) by the following consecutive steps: (i) hydrogen abstraction from the enolate form of AA or MAA by ferrylMb yielding a resonance-stabilized enoyl radical at the substrate C2; (ii) oxygen addition to the substrate radical intermediate to form the respective α-peroxyl $AAOO^{\bullet}$ and $MAAOO^{\bullet}$ radicals; (iii) reaction propagation by the alkylperoxyl radicals yielding AA or MAA α-hydroperoxides until dissolved oxygen depletion; (iv) α-hydroperoxide cyclization to the corresponding dioxetanones, whose thermal cleavage produces methylglyoxal or diacetyl, respectively, in the electronically excited triplet state; and (v) triplet carbonyl decay by light emission, deactivation by solvent, and quenching by oxygen to their ground state or Norrish cleavage to acetyl radicals are competing processes that destroy the excited product.

β-Dicarbonyl compounds and β-ketoacids and esters have long been known to exist in aqueous medium in a phosphate-catalyzed dynamic equilibrium with their enolic forms, stabilized by an intramolecular hydrogen bond (Scheme 1). Consequently, the enolization constants of β-dicarbonyls (e.g., ethyl acetoacetate, $K_e = 0.053$; acetoacetone, $K_e = 0.34$) [53] are much higher than those of monoketones (e.g., acetone, $K_e = 6.0 \times 10^{-9}$) [54], or monoaldehydes (e.g., isobutanal, $K_e = 1.7 \times 10^{-4}$) [55]. In addition, α-alkylation of enols and phenols renders them more prone to electron donation. Thus, the oxidation potential of pentan-2-one, pentan-2,4-dione (acetoacetone), and 3-methylpentan-2,4-dione (3-methylacetoacetone) decreases in this same order [56]. Therefore, the ease of both enolization and one-electron oxidation is expected to contribute to the reactivity of carbonyl compounds with oxygen initiated by peroxidase-acting hemeproteins in the presence of peroxides. Accordingly, isobutanal [57] and 3-methylacetoacetone [58] were unequivocally shown to yield acetone and diacetyl, respectively, in the triplet state, when treated in aerated phosphate buffer with HRP (horseradish peroxidase) in the presence of traces of peroxides. Formation of these products was supported by the complete matching of the chemiluminescence spectrum of the isobutanal or 3-methylacetoacetone reaction with the phosphorescence spectra of acetone and diacetyl, respectively. Triplet carbonyls are potentially biological toxicants due to their chemical reactivity, similar to that of alkoxyl radicals [33]: hydrogen abstraction from polyunsaturated fatty acids, isomerization, cleavage to radicals, and addition to double bonds, for example. In addition, triplet carbonyls can transfer electronic energy to ground state oxygen yielding the very highly electrophilic excited O_2 ($^1\Delta_g$) [59].

Here, methylglyoxal-generating and oxygen-consuming AA was also shown to be chemiluminescent in the presence of Mb/H_2O_2 (Figs. 2, 7, and 10), which may attest to the intermediacy of a dioxetane-type intermediate. That ferrylMb acts as an electron acceptor from AA and MAA is demonstrated by DMPO immunospin

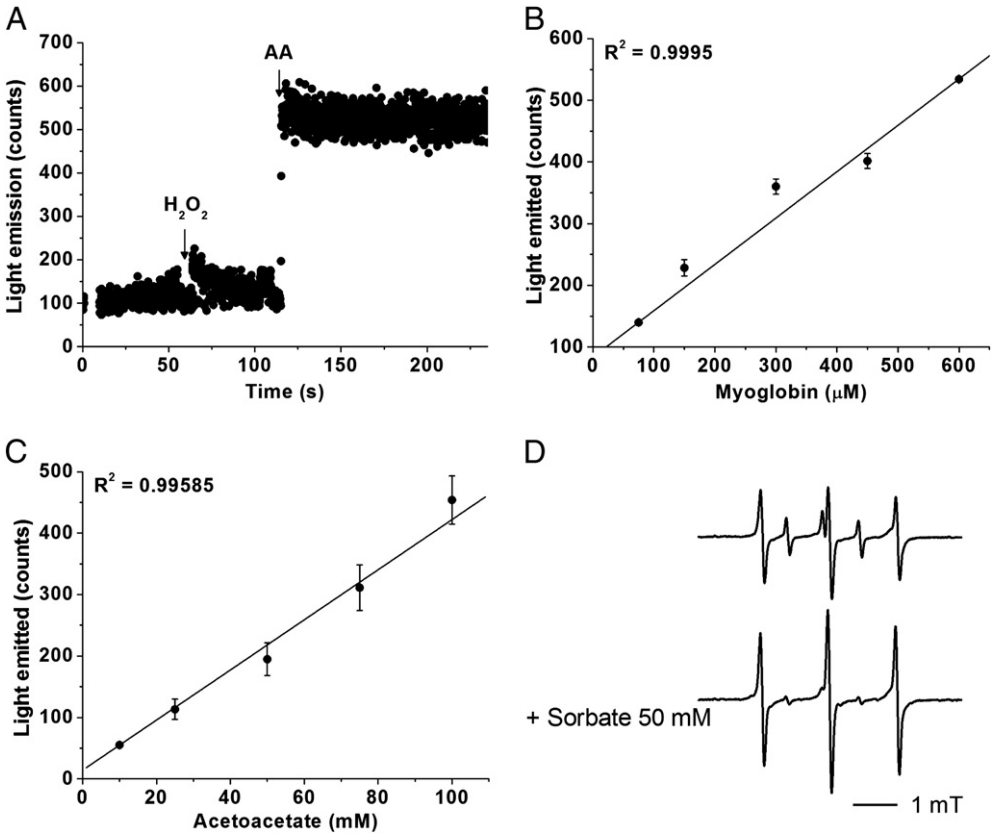

Fig. 10. Ultraweak chemiluminescence elicited by the AA/Mb/H_2O_2 system. (A) Temporal course of light emission from Mb (500 μM) and H_2O_2 1:1 (500 μM) with added AA (100 mM). (B and C) Dose-dependent light intensity vs AA and Mb concentrations, respectively. (D) Quenching effect of sorbate (50 mM) on the MNP-acetyl radical adduct EPR signal observed with Mb (250 μM) added to H_2O_2 1:100 (25 mM) and MAA (50 mM) in the presence of MNP (50 mM). Other experimental conditions were as described under Materials and methods.

trapping (Fig. 1B) and the importance of the ratio of Mb:H_2O_2 in product yields and radical intermediate production (Figs. 8 and 9). The intermediacy of resulting AA-secondary carbon radical (Figs. 3 and 4 and Table 1) and the MAA-tertiary radical (Fig. 5) centered at carbon 2 was obtained by EPR spin trapping with MNP, combined with isotopic labeling in the case of AA (Fig. 4). The EPR spin-trapping studies revealed the presence of the distinctive acetyl radical MNP adduct (Figs. 5 and 9) in the reaction mixture containing MAA, probably formed by Norrish cleavage of triplet diacetyl formed from the dioxetanone intermediate of the substrate oxidation. Accordingly, the signal of the MNP-acetyl radical adduct was quenched on addition of sorbic acid (Fig. 10), a well-known conjugated diene that acts as a collisional quencher of triplet ketones [52].

Table 1
Hyperfine coupling constants (mT) of the MNP radical adducts obtained from AA and MAA oxidized by the Mb/H_2O_2 system in aerated 100 mM phosphate buffer, pH 7.4, at 25 °C.

	a^N	a^H_β	a^{13C}_α	a^{13C}_β	a^{13C}_γ
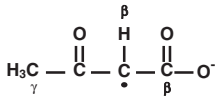	1.458	0.334	0.68	1.284	0.076
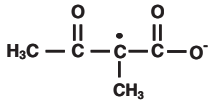	1.58				
	0.83				

Product analysis and kinetics data showed that MAA is about one order of magnitude more reactive than AA for oxidation by the Mb/H_2O_2 system (Figs. 6 and 7), as predicted by the effect of α-methylation that makes MAA easier to be oxidized [17,46,56]. Replacement of H_2O_2 by *tert*-butOOH to produce ferrylMb corroborated these data (not shown).

The role of ferrylMb as initiator of the oxygen-consuming reaction of AA and MAA was shown here by the spectrophotometric detection of heme hyperoxidation and by an immunospin-trapping experiment which detects the primary Mb Tyr 103 radical (Fig. 1). Accordingly, the pH profiles of oxygen consumption and diacetyl production by the Mb/H_2O_2-catalyzed oxidation of MAA revealed that the reaction rates are higher at lower pH, as expected for ferrylMb acting as the primary one-electron oxidant of the β-ketoacid (Fig. 8). When higher amounts of H_2O_2 were added (Mb:H_2O_2>1:25) (Figs. 7 and 9), the yield of products and of substrate radicals decreased significantly, which was attributed to the observed bleaching and destruction of the hemeprotein (data not shown).

Biological implications

The findings of the present work alert us to the potential adverse effects of peroxidase-acting Mb in ketogenesis. For example, ketogenesis is largely accepted as a risk factor for rhabdomyolysis due to osmotic imbalance [60–62], but there may also be a contribution from free radicals, reactive α-dicarbonyl products, and excited states generated by Mb-catalyzed peroxidation of β-ketoacids such as AA

and MAA. Carbon-centered radicals and triplet methylglyoxal produced by Mb/peroxide acting as a peroxidase on AA have the potential to modify a large spectrum of biomolecules. Furthermore, methylglyoxal is an α-oxoaldehyde that is extremely reactive with amino groups of proteins by virtue of the electron-withdrawing effect from a neighboring carbonyl group, leading to advanced glycated end products, such as ε-carboxyethyl lysine (CEL) and methylglyoxal-derived lysine dimer (MOLD) [63]. These carbonyl adducts accumulate and are proposed as biomarkers in age-related diseases such as diabetes [64], uremia [65], Alzheimer's [66], atherosclerosis [67], and aging [68]. It is tempting to propose that the Mb-catalyzed oxidation of AA operates in ketoacidotic patients, and is thus responsible for the higher methylglyoxal levels detected in plasma from these patients [18].

Receptors for AGEs, named RAGEs, have been shown to be involved in the development of macro and microvascular diseases associated with diabetes and aging [21,28,29], where α-dicarbonyl catabolite Schiff reactions with protein amino acid residues have been implicated. In conclusion, we hypothesize here that Mb and other peroxidase-acting hemeproteins induce the aerobic oxidation of β-ketoacids accumulated in ketoacidosis, yielding reactive radicals, α-dicarbonyls, and excited triplet species which spark adverse biological responses.

Acknowledgments

This work was supported by grants from the Fundação de Amparo à Pesquisa do Estado de São Paulo (FAPESP), the Conselho Nacional de Desenvolvimento Científico e Tecnológico (CNPq), the Instituto Nacional de Ciência e Tecnologia (INCT) Redoxoma, and Intramural Research Program of the National Institute of Environmental Health Sciences (NIEHS). We acknowledge Dr. Ann Motten for editing this manuscript.

References

[1] Jain, S. K.; Mc Vie, R.; Bocchini Jr., J. A. Hyperketonemia (ketosis), oxidative stress and type 1 diabetes. *Pathophysiology* **13:**163–170; 2006.
[2] Goto, K.; Ishii, N.; Mizuno, A.; Takamatsu, K. Enhancement of fat metabolism by repeated bouts of moderate endurance exercise. *J. Appl. Physiol.* **102:**2158–2164; 2007.
[3] Adam-Perrot, A.; Clifton, P.; Brouns, F. Low-carbohydrate diets: nutritional and physiological aspects. *Obesity Rev.* **7:**49–58; 2006.
[4] Kornman, S. H. Inborn errors of isoleucine degradation: a review. *Mol. Genet. Metab.* **89:**289–299; 2006.
[5] Aramaki, S.; Lehotay, D.; Sweetman, L.; Nyhan, W. L.; Winter, S. C.; MmDleton, B. Urinary excretion of 2-methylacetoacetate, 2-methyl-3-hydroxybutyrate and triglylglycine after isoleucine loading in the diagnosis of 2-methylacetoacetyl-CoA thiolase deficiency. *J. Inherit. Metab. Dis.* **14:**63–74; 1991.
[6] Rosa, R. B.; Schuck, P. F.; de Assis, D. R.; Latini, A.; Dalcin, K. B.; Ribeiro, C. A.; da S. Ferreira, G.; Maria, R. C.; Leipnitz, G.; Perry, M. L.; Filho, C. S.; Wyse, A. T.; Wannmacher, C. M.; Wajner, M. Inhibition of energy metabolism by 2-methylacetoacetate and 2-methyl-3-hydroxybutyrate in cerebral cortex of developing rats. *J. Inherit. Metab. Dis.* **28:**501–515; 2005.
[7] Jain, S. K.; Kannan, K.; Lim, G.; McVie, R.; Bocchini Jr., J. A. Hyperketonemia increases tumor necrosis factor-alpha secretion in cultured U937 monocytes and Type 1 diabetic patients and is apparently mediated by oxidative stress and cAMP deficiency. *Diabetes* **51:**2287–2293; 2002.
[8] Jain, S. K.; Kannan, K.; MacVie, R. Effect of hyperketonemia on blood monocytes in type-I diabetic patients and apoptosis in cultured U937 monocytes. *Antioxid. Redox. Signal.* **1:**211–220; 1999.
[9] Jain, S. K.; Kannan, K.; Lim, G.; Matthews-Greer, J.; McVie, R.; Bocchini Jr., J. A. Elevated blood interleukin-6 levels in hyperketonemic type 1 diabetic patients and secretion by acetoacetate-treated cultured U937 monocytes. *Diabetes Care* **26:**2139–2143; 2003.
[10] Abdelmegeed, M. A.; Kim, S. K.; Woodcroft, K. J.; Novak, R. F. Acetoacetate activation of extracellular signal-regulated kinase 1/2 and p38 mitogen-activated protein kinase in primary cultured rat hepatocytes: role of oxidative stress. *J. Pharmacol. Exp. Ther.* **310:**728–736; 2004.
[11] Jain, S. K.; Kannan, K.; Lim, G. Ketosis (acetoacetate) can generate oxygen radicals and cause increased lipid peroxidation and growth inhibition in human endothelial cells. *Free Radic. Biol. Med.* **25:**1083–1088; 1998.
[12] Juge, N.; Gray, J. A.; Omote, H.; Miyaji, T.; Inoue, T.; Hara, C.; Uneyama, H.; Edwards, R. H.; Nicoll, R. A.; Moriyama, Y. Acetoacetate protects neuronal cells from oxidative glutamate toxicity. *Neuron* **68:**99–112; 2010.
[13] Mallet, R. T.; Sun, J. Antioxidant properties of myocardial fuels. *Mol. Cell. Biochem.* **253:**103–111; 2003.
[14] Kushnareva, Y.; Murphy, N. A.; Andreyev, A. Complex I-mediated reactive oxygen species generation: modulation by cytochrome c and NAD(P)$^+$ oxidation-reduction state. *Biochem. J.* **368:**545–553; 2002.
[15] Vidigal, C. C.; Cilento, G. Evidence for the generation of excited methylglyoxal in the myoglobin catalyzed oxidation of acetoacetate. *Biochem. Biophys. Res. Commun.* **62:**184–190; 1975.
[16] Harrison, J. E.; Saeed, F. A. Acetoacetate is an electron donor to myeloperoxidase and a promoter of myeloperoxidase-catalyzed fatty acid peroxidation. *Biochem. Med.* **26:**339–355; 1981.
[17] Royer, L. O.; Knudsen, F. S.; de Oliveira, M. A.; Tavares, M. F.; Bechara, E. J. Peroxynitrite-initiated oxidation of acetoacetate and 2-methylacetoacetate esters by oxygen: potential sources of reactive intermediates in ketoacidoses. *Chem. Res. Toxicol.* **17:**1725–1732; 2004.
[18] Turk, Z.; Nemet, I.; Varga-Defteardarović, L.; Car, N. Elevated level of methylglyoxal during diabetic ketoacidosis and its recovery phase. *Diabetes Metab.* **32:**176–180; 2006.
[19] Thornalley, P. Dicarbonyl intermediates in the Maillard reaction. *Ann. N. Y. Acad. Sci.* **1043:**111–117; 2005.
[20] Thornalley, P. Protein and nucleotide damage by glyoxal and methylglyoxal in physiological systems—role in ageing and disease. *Drug Metab. Drug Interact.* **23:**125–150; 2008.
[21] Fleming, T. H.; Humpert, P. M.; Nawroth, P. P.; Bierhaus, A. Reactive metabolites and AGE/RAGE-mediated cellular dysfunction affect the aging process—a mini-review. *Gerontology* (21 October 2010). Electronic publication ahead of print.
[22] Desai, K. M.; Chang, T.; Wang, H.; Banigesh, A.; Dhar, A.; Liu, J.; Untereiner, A.; Wu, L. Oxidative stress and aging: is methylglyoxal the hidden enemy? *Can. J. Physiol. Pharmacol.* **88:**273–284; 2010.
[23] Ramasamy, R.; Yan, S. F.; Schmidt, A. M. Advanced glycation endproducts: from precursors to RAGE: round and round we go. *Amino Acids.* (19 October 2010).
[24] Karashalias, N.; Babaei-Jadidi, R.; Rabbani, N.; Thornalley, P. J. Increased protein damage in renal glomeruli, retina, nerve, plasma and urine and its prevention by thiamine and benfotiamine therapy in a rat model of diabetes. *Diabetologia* **53:**1506–1516; 2010.
[25] Nangaku, M.; Miyata, T.; Sada, T.; Mizuno, M.; Inagi, R.; Ueda, Y.; Ishikawa, N.; Yuzawa, H.; Koike, H.; van Ypersele de Strihou, C.; Kurokawa, K. Anti-hypertensive agents inhibit in vivo the formation of advanced glycation end products and improve renal damage in a type 2 diabetic nephropathy rat model. *J. Am. Soc. Nephrol.* **14:**1212–1222; 2003.
[26] Nangaku, M.; Izuhara, Y.; Usuda, N.; Inagi, R.; Shibata, T.; Sugiyama, S.; Kurokawa, K.; van Ypersele de Strihou, C.; Miyata, T. In a type 2 diabetic nephropathy rat model, the improvement of obesity by a low calorie diet reduces oxidative/carbonyl stress and prevents diabetic nephropathy. *Nephrol. Dial. Transplant.* **20:**2661–2669; 2005.
[27] Mostaf, A. A.; Randell, E. W.; Vasdev, S. C.; Gill, V. D.; Han, Y.; Gadag, V.; Raouf, A. A.; El Said, H. Plasma protein advanced glycation end products, carboxymethyl cysteine, and carboxyethyl cysteine, are elevated and related to nephropathy in patients with diabetes. *Mol. Cell. Biochem.* **302:**35–42; 2007.
[28] Reiniger, N.; Lau, K.; McCalla, D.; Eby, B.; Cheng, B.; Lu, Y.; Qu, W.; Quadri, N.; Ananthakrishnan, R.; Furmansky, M.; Rosario, R.; Song, F.; Rai, V.; Weinberg, A.; Friedman, R.; Ramasamy, R.; D'Agati, V.; Schmidt, A. M. Deletion of the receptor for advanced glycation end products reduces glomerulosclerosis and preserves renal function in the diabetic OVE26 mouse. *Diabetes* **59:**2043–2054; 2010.
[29] Liu, Y.; Liang, C.; Liu, X.; Pan, X.; Ren, Y.; Fan, M.; Li, M.; He, Z.; Wu, J.; Wu, Z. AGEs increased migration and inflammatory responses of adventitial fibroblasts via RAGE. MAPK and NF-kappaB pathways. *Atherosclerosis* **208:**34–42; 2010.
[30] Giulivi, C.; Cadenas, E. Ferrylmyoglobin: formation and chemical reactivity toward electron-donating compounds. *Methods Enzymol.* **233:**189–202; 1994.
[31] Gunther, M. R.; Sturgeon, B. E.; Mason, R. P. A long-lived tyrosyl radical from the reaction between horse metmyoglobin and hydrogen peroxide. *Free Radic. Biol. Med.* **28:**709–719; 2000.
[32] DeGray, J. A.; Gunther, M. R.; Tschirret-Guth, R.; Ortiz de Montellano, P. R.; Mason, R. P. Peroxidation of a specific tryptophan of metmyoglobin by hydrogen peroxide. *J. Biol. Chem.* **272:**2359–2362; 1997.
[33] Cilento, G.; Adam, W. From free radicals to electronically excited species. *Free Radic. Biol. Med.* **19:**103–114; 1995.
[34] Moore, K. P.; Holt, S. G.; Patel, R. P.; Svistuneko, D. A.; Zackert, W.; Goodier, D.; Reeder, B. J.; Clozel, M.; Anand, R.; Cooper, C. E.; Morrow, J. D.; Wilson, M. T.; Darley-Usmar, V.; Roberts II, L. J. A causative role for redox cycling of myoglobin and its inhibition by alkalinization in the pathogenesis and treatment of rhabdomyolysis-induced renal failure. *J. Biol. Chem.* **273:**31731–31737; 1998.
[35] Noble, R. W.; Gibson, Q. H. The reaction of ferrous horseradish peroxidase with hydrogen peroxide. *J. Biol. Chem.* **245:**2409–2413; 1970.
[36] Krebs, H. A.; Eggleston, L. V. Metabolism of acetoacetate in animal tissues 1. *Biochem. J.* **39:**408–419; 1945.
[37] Hardman, K. D.; Eylar, E. H.; Ray, D. K.; Banaszak, L. J.; Gurd, F. R. N. Isolation of sperm whale myoglobin by low temperature fractionation with ethanol and metallic ions. *J. Biol. Chem.* **241:**432–442; 1966.
[38] Robinson, J.; Cooper, J. M. Method of determining oxygen concentration in biological media, suitable for calibrations of the oxygen electrode. *Anal. Biochem.* **33:**390–399; 1970.
[39] Mottley, C.; Robinson, R. E.; Mason, R. P. Free radical formation in the oxidation of malondialdehyde and acetylacetone by peroxidase enzymes. *Arch. Biochem. Biophys.* **15:**153–160; 1991.
[40] Bednarski, W.; Jedrychowski, L.; Hammond, E. G.; Nikolov, Z. L. A method for the determination of α-dicarbonyl compounds. *J. Dairy Sci.* **72:**2474–2477; 1989.

[41] Ferreira, A. C. S.; Reis, S.; Rodrigues, C.; Oliveira, C.; Pinho, P. G. Simultaneous determination of ketoacids and dicarbonyl compounds, key Maillard intermediates on the generation of aged wine aroma. *J. Food Sci.* **72:**S314–S318; 2007.
[42] Takagi, M.; Ono, S. Polarigraphic studies on quinoxalines for the determination of carbonyl groups in starches. *Bull. Univ. Osaka Pref., Ser. B* **21:**77–122; 1969.
[43] Walker, P. G. *A colorimetric method for the estimation of acetoacetate. Biochem. J.* **58:** *699–704; 1954.*
[44] Wolff, S. P. Ferrous ion oxidation in presence of ferric ion indicator xylenol orange for measurement of hydroperoxides. *Methods Enzymol.* **233:**182–189; 1994.
[45] Bou, R.; Codony, E.; Tres, A.; Decker, E. A.; Guardiola, F. Determination of hydroperoxides in foods and biological samples by the ferrous oxidation-xylenol orange method: a review of the factors that influence the method's performance. *Anal. Biochem.* **377:**1–15; 2008.
[46] Knudsen, F. S.; Penatti, C. A.; Royer, L. O.; Bidart, K. A.; Christoff, M.; Ouchi, D.; Bechara, E. J. Chemiluminescent aldehyde and beta-diketone reactions promoted by peroxynitrite. *Chem. Res. Toxicol.* **13:**317–326; 2000.
[47] Mottley, C.; Robinson, R. E.; Mason, R. P. Free radical formation in the oxidation of malondialdehyde and acetylacetone by peroxidase enzymes. *Arch. Biochem. Biophys.* **289:**153–160; 1991.
[48] Bechara, E. J.; Dutra, F.; Cardoso, V. E.; Sartori, A.; Olympio, K. P.; Penatti, C. A.; Adhikari, A.; Assunção, N. A. The dual face of endogenous alpha-aminoketones: pro-oxidizing metabolic weapons. *Comp. Biochem. Physiol. C Toxicol. Pharmacol.* **146:**88–110; 2007.
[49] Silaghi-Dumitrescu, R.; Reeder, B. J.; Nicholls, P.; Cooper, C. E.; Wilson, M. T. Ferryl haem protonation gates peroxidatic reactivity in globins. *Biochem. J.* **403:**391–395; 2007.
[50] Adam, W.; Sternmetzer, H. C. *(1-Adamantyl)-α-peroxylactone: synthesis, kinetics, and luminescence. Angew. Chem. Int. Ed. Engl.* **11:***540–542; 1972.*
[51] Kopecky, K. L.; Mumford, C. Luminescence in the thermal decomposition of 3,3,4-trimethyl-1,2-dioxetane. *Can. J. Chem.* **47:**709; 1969.
[52] Velosa, A. C.; Baader, W. J.; Stevani, C. V.; Mano, C. M.; Bechara, E. J. 1,3-diene probes for detection of triplet carbonyls in biological systems. *Chem. Res. Toxicol.* **20:**1162–1169; 2007.
[53] Iglesias, E. *Determination of keto–enol equilibrium constants and the kinetic study of the nitrosation reaction of β-dicarbonyl compounds. J. Chem. Soc., Perkin Trans. 2* **3:** *431–439; 1997.*
[54] Chiang, Y.; Kresge, A. J.; Tang, Y. S.; Wirz, J. The pKa, and keto-enol equilibrium constant of acetone in aqueous solution. *J. Am. Chem. Soc.* **106:**460–462; 1984.
[55] Bohne, C.; MacDonald, D.; Dunford, B. Transient state kinetics of the reactions of isobutyraldehyde with compounds I and II of horseradish peroxidase. *J. Biol. Chem.* **262:**3572–3578; 1987.
[56] Adkins, H.; Cox, F. W. Relative oxidation-reduction reactivities of ketones and aldehydes and applications in synthesis. *J. Am. Chem. Soc.* **60:**1151–1159; 1938.
[57] Indig, G.; Campa, A.; Bechara, E. J. H.; Cilento, G. Conjugate diene formation promoted by triplet acetone acting on arachidonic acid. *Photochem. Photobiol.* **48:** 719–723; 1988.
[58] Soares, C.; Bechara, E. Enzymatic generation of triplet biacetyl. *Photochem. Photobiol.* **36:**117–119; 1982.
[59] Wilkinson, F.; McGarvey, D. J.; Olea, A. F. Excited triplet state interactions with molecular oxygen: influence of charge transfer on the bimolecular quenching rate constants and the yields of singlet oxygen ($1\Delta g$) for substituted naphthalenes in various solvents. *J. Phys. Chem.* **98:**3762–3769; 1994.
[60] Cervellin, G.; Comelli, I.; Lippi, G. Rhabdomyolysis: historical background, clinical, diagnostic and therapeutic features. *Clin. Chem. Lab. Med.* **48:**749–756; 2010.
[61] Tanaka, M.; Miyazaki, Y.; Ishikawa, S.; Matsuyama, K. Alcoholic ketoacidosis associated with multiple complications: report of 3 cases. *Intern. Med.* **43:** 955–959; 2004.
[62] Casteels, K.; Beckers, D.; Wouters, C.; Van Geet, C. Rhabdomyolysis in diabetic ketoacidosis. *Pediatr. Diabetes* **4:**29–31; 2003.
[63] Degenhardt, T. P.; Thorpe, S. R.; Baynes, J. W. Chemical modification of proteins by methylglyoxal. *Cell Mol. Biol. (Noisy-le-grand)* **44:**1139–1145; 1998.
[64] Jakus, V.; Riebrock, N. Advanced glycation end-products and the progress of diabetic vascular complications. *Physiol. Res.* **53:**131–142; 2004.
[65] Semba, R. D.; Fink, J. C.; Sun, K.; Bandinelli, S.; Guralnik, J. M.; Ferrucci, L. Carboxymethyl-lysine, an advanced glycation end product, and decline of renal function in older community-dwelling adults. *Eur. J. Nutr.* **48:**38–44; 2009.
[66] Sato, T.; Shimogaito, N.; Wu, X.; Kikuchi, S.; Yamagishi, S.; Takeuchi, M. Toxic advanced glycation end products (TAGE) theory in Alzheimer's disease. *Am. J. Alzheimers Dis. Other Demen.* **21:**197–2008; 2006.
[67] Kislinger, T.; Fu, C.; Huber, B.; Qu, W.; Taguchi, A.; Du Yan, S.; Hofmann, M.; Yan, S. F.; Pischetsrieder, M.; Stern, D.; Schmidt, A. M. *N*(epsilon)-(carboxymethyl) lysine adducts of proteins are ligands for receptor for advanced glycation end products that activate cell signaling pathways and modulate gene expression. *J. Biol. Chem.* **274:**31740–31749; 1999.
[68] Schlotterer, A.; Kukudov, G.; Bozorgmehr, F.; Hutter, H.; Du, X.; Oikonomou, D.; Ibrahim, Y.; Pfisterer, F.; Rabbani, N.; Thornalley, P.; Sayed, A.; Fleming, T.; Humpert, P.; Schwenger, V.; Zeier, M.; Hamann, A.; Stern, D.; Brownlee, M.; Bierhaus, A.; Nawroth, P.; Morcos, M. *C. elegans* as model for the study of high glucose-mediated life span reduction. *Diabetes* **58:**2450–2456; 2009.